O.E.C.D. HIGH TEMPERATURE REACTOR PROJECT

DRAGON

Dragon Project Report

DIMENSIONAL CHANGES OF GRAPHITE SPECIMENS IRRADIATED IN DRAGON FUEL ELEMENT 700

PART II

SOME COMMENTS ON THE IRRADIATION SHRINKAGE OF GRAPHITE

by

M. R. EVERETT
L. W. GRAHAM

A.E.E. Winfrith, Dorchester, Dorset, England
November, 1967

DIMENSIONAL CHANGES OF GRAPHITE SPECIMENS IRRADIATED IN DRAGON FUEL ELEMENT 700

PART II

SOME COMMENTS ON THE IRRADIATION SHRINKAGE OF GRAPHITE

by

M. R. EVERETT

L. W. GRAHAM

ABSTRACT

Although the qualitative mechanism of irradiation damage and dimensional change of graphite crystallites is quite well understood, the existing quantitative theories do not predict the irradiation shrinkage behaviour of a range of graphites with very good accuracy. It is suggested that this is because the effects of crystallite height, crystallite diameter crystallite shape and crystallite mechanical properties such as the shear modulus are not considered with respect to the magnitude of crystallite/crystallite dimensional interactions. A model which takes into account these effects is developed and the associated physical property parameter correlated against the initial irradiation volume shrinkage rates of fourteen different graphites. It is considered more logical that the volume change of a graphite should be first understood and the anisotropy taken into account at a later stage.

CONTENTS

LIST OF TABLES

LIST OF ILLUSTRATIONS

FIGURE

DIMENSIONAL CHANGES OF GRAPHITE SPECIMENS IRRADIATED IN DRAGON FUEL ELEMENT 700

PART II

SOME COMMENTS ON THE IRRADIATION SHRINKAGE OF GRAPHITE

by

M. R. EVERETT

L. W. GRAHAM

1. INTRODUCTION

In designing a high temperature gas cooled nuclear reactor it is necessary to know the extent to which graphite components of the fuel elements and moderator deform when exposed at temperatures in the range 350°C to 1400°C to fast neutron doses of at least 3×10^{22} n cm^{-2} (Ni dose Dido). It is also highly desirable to understand as fully as possible the mechanism of irradiation shrinkage in graphite to provide confidence in design and control over material quality.

At present there are two main classifications of theoretical models for graphite irradiation shrinkage. The "two-phase" theory advanced by De Halas and Yoshikawa [1] maintains that at temperatures above 500°C the dimensional changes of graphite are strongly influenced by the shrinkage of a relatively small proportion of poorly graphitised material and that the dimensional changes of the crystallites are not the main controlling factor. This two-phase theory has not been put into quantitative terms but papers by Morgan [2] have discussed further the qualitative application of the theory.

The "single-phase" theory considers that the dimensional behaviour of graphite can be ascribed wholly to the dimensional changes of the crystallites (i.e., the largest unit of the graphite structure which can be taken to exhibit reasonable single crystal properties). Simmons [3] has used the coefficients of thermal expansion (α_x) of a graphite in a given direction of cut, to relate the anisotropy of the bulk material to relative contributions of c-axis and a-axis crystallite character.

$$\alpha_x = A_x \alpha_c + (1 - A_x) \alpha_a \qquad (1)$$

where α_c and α_a are the thermal expansion coefficients of a single crystal of graphite in the c and a-axis directions respectively. The factor A_x is a parameter characteristic of the specimen dependent on the orientation indicated by direction x in Equation (1). This same factor A_x is used in a second equation in a similar manner to describe the relative contributions of c-axis and a-axis single crystal expansions or contractions to the dimensional change of the graphite under irradiation.

$$X_x = A_x X_c + (1 - A_x) X_a$$

where:

X_x = rate of dimensional change of the bulk graphite dose in the x direction of the material, per unit neutron dose.

X_c = rate of dimensional change of a crystallite in the c-axis direction, per unit neutron dose.

X_a = rate of dimensional change per unit neutron dose of a crystallite in the a-axis direction, per unit neutron dose.

An alternative treatment of the single phase theory developed by Price and Bokros [4] has been referred to as a "crystallite averaging" model which utilises a preferred orientation parameter derived from X-ray diffraction measurements and an accommodation coefficient which takes into account the accommodation of c-axis expansion by basal plane "Mrozowski" microcracks.

A recent series of experiments by Price and Bokros [5] has tested the validity of the two single-phase theories. Both theories satisfactorily relate the direction of cut of a sample of an anisotropic graphite to its irradiation shrinkage over a range of temperatures, by means of accommodation coefficients derived as indicated above.

From extensive work carried out on PGA graphite the application of the Simmons equations has enabled Bridge, et al., [6] and Graham [7] to calculate the rates of c-axis and a-axis dimensional changes occurring in the crystallites in PGA graphite. This data has been combined and is shown in Fig. 1. If applied to PGA graphite and to some other graphites of similar properties, this data satisfactorily explains the initial dimensional changes of the bulk material under irradiation. For other graphites however, the Simmons equations do not predict the rates of dimensional change at all satisfactorily as will be shown later.

There is no reason to suppose that these latter graphites are in any way less graphitic; in many cases the basic materials are the same but the product has different physical properties. This is particularly apparent with the isotropic graphites based on "Gilsonite" (a coke made from naturally occurring spherical pitch globules) and which has a spherical arrangement of its component crystallites and therefore it must be assumed that the crystallites in slightly dissimilar graphites can produce different bulk dimensional change effects.

This type of anomaly has prompted a consideration of whether the existing graphite irradiation theories account for the dimensional changes of graphite in the way that is required, for example there is perhaps too great an emphasis on the study of initial shrinkage behaviour and bulk anisotropy. Do the theories realistically take into account the way in which a crystallite interacts with its neighbour dimensionally bearing in mind that this property may vary with the nature of the graphite?

In a companion study in which graphites have been irradiated at high temperatures it has already been suggested that irradiation induced dimensional changes are profoundly influenced by mechanical interactions

between crystallites even at low doses, leading to indications that the bulk dimensional changes may be correlated with the initial elastic properties rather than the coefficient of thermal expansion [7]. It is the purpose of this paper to develop this hypothesis in the light of the material properties of a range of graphites and the dimensional changes found on irradiating specimens in the Dragon Reactor. The experimental details and results are presented in full elsewhere [10].

2. THEORETICAL MODEL FOR CRYSTALLITE/CRYSTALLITE INTERACTION

When a graphite is cooled from its graphitisation temperature of 2700-2800°C to a temperature in the region of 2000°C the shape changes of the crystallites caused by the high ratio of c-axis shrinkage to a-axis shrinkage is supposed to be accommodated by creep or plastic deformation of the crystallites. Below the temperature of ~2000°C, data by Nelson and Riley [8] suggests that when a graphite crystal is cooled to say 500°C the average ratio of c-axis contraction to a-axis contraction is of the order of 30. The graphite cannot adequately accommodate those local dimensional changes by plastic deformation and "Mrozowski" microcracks parallel to the basal plane are opened up. This c-axis shrinkage is of the order of 5% of the average crystal height (L_c) found in a graphite at room temperature.

In any random arrangement of anisotropic crystallites the "shapes" of the crystallites must play an important part. If all the crystallites have plane surfaces at right angles to the a, b and c axes a reasonably simple form of shrinkage can be envisaged which is dominated by the slowest shrinking axes of the crystallites, i.e., the a and b axes. This type of system would have a reasonably perfect form of c-axis expansion accommodation when the graphite is heated; the interference of one crystallite with its neighbour is small. It is obvious however that in practice whilst reasonably planer surfaces can be expected parallel to the basal plane because of the ease of cleavage, the surfaces at right angles to the basal plane will be characterised by a range of angles and the interaction of one crystallite upon its neighbour must be considered from a dimensional point of view. This point can best be illustrated by reference to a simple two dimensional case. In Fig. 2(a) the thermal contraction deformation of a crystallite of square section P_0 Q_0 R S at 2000°C is exaggerated and shown as P_1 Q_1 R S at 500°C with point R, i.e., a corner of the crystal acting as a fixed point. If the space P_0 Q_0 R S is considered to be that available to the crystallite - the movement of adjacent crystallite surfaces is ignored in this simple illustration - a simple microcrack bounded by P_0 P_1 S_1 S_0 is opened up and the a-axis shrinkage from the line P_0 Q to P_1 Q_1 is the limiting dimension in an array of such crystallites. If point R is fixed and the crystallite irradiated at 500°C the shape change is represented by P_5 Q_5 R S_5, etc., if the crystallite dimensional changes shown in Fig. 1 are accepted.

If however a crystallite of rhombohedral section (a rhombohedral section has been chosen purely to illustrate the two cases which arise when θ is $<90^\circ$ or $>90^\circ$) is considered in a similar manner as in Fig. 2(b) it is seen that on thermal shrinkage the point P_1 intrudes into the space allocated to adjacent crystallites. A stress is raised in the rhombohedral crystallite, as shown

by the two arrows, which can be relieved by:

(a) shear in the crystallite

(b) strain in the crystallite

(c) rotation of the crystallite in an anti-clockwise direction, or

(d) a microcrack parallel to $P_0\ Q_0$.

Obviously in an actual case the crystallite is not free to position itself such that point R acts as a fixed point, there will be restraints arising from bonds or other interactions with adjacent crystallites which limit the extent by which the stress in the crystallite is relieved by the processes (a), (b), (c) and (d) above. In an actual graphite there will be a number of crystallite/crystallite interaction geometries where no interference takes place (e.g., the face RS in Fig. 2(b)) but in a system with a random arrangement of a range of crystallite sizes and shapes the effect illustrated by the right-hand side of Fig. 2(b) must predominate, i.e., the positive interferences will exceed in magnitude the negative interference effects illustrated on the left-hand side of Fig. 2(b). The movement of point P_0 at the edge of a crystallite with angle $\theta < 90^\circ$ and in contact with an adjacent crystallite surface $R_0\ Q_0$ is considered in a little more detail in Fig. 3. On cooling to 500°C the point P will lie somewhere on the line $P_1\ P_1'$ depending upon the degree and combination of shear, strain or rotation which has taken place in the crystallite or alternatively whether the crystallite has displaced the surface $R_0\ Q_0$ to $R_1\ Q_1$.

When the crystallite is irradiated (successive neutron doses are indicated by the series of subscripts), the point P will follow a path as follows:

(i) $P_1\ P_2\ P_3\ \ldots$ if no crystallite strain takes place; the displaced adjacent crystallite surface $Q_1\ R_1$ will approach $Q_0\ R_0$ and the graphite shrinks

(ii) $P_1'\ P_2'\ P_3'\ \ldots$ if the crystallite has sustained full strain or shear, in which case no displacement of surface $Q_1\ R$ of the adjacent crystallite will have taken place and little or no dimensional change will result in the graphite.

These two cases are extremes and the practical case will lie between the two. In effect the rate of a-axis shrinkage transmitted from the crystallite to its neighbour will initially be small and will increase until the point P_6 is reached - here the crystallite shape will be the nearest approach to the original 2000°C case; the system will have minimum strain energy and the full rate of a-axis shrinkage can now be transmitted to the adjacent crystallite until the point P approaches the line P_0-P_{16} which represents closure of the basal plans microcrack, thus producing an increase in the rate of shape change of the crystallite and causing another stress system to be set up.

This model suggests that a low rate of irradiation shrinkage will be obtained if:

(a) The crystallite height (L_c) is small; thus reducing the magnitude of crystallite/crystallite interference effects.

(b) The crystallite diameter (L_a) is large thus reducing the number of crystallite/crystallite interferences and also providing slower rates of crystallite dimensional change arising from enhancement of interstitial-vacancy annihilation.

(c) The Young's modulus of the crystallites is low thus permitting strain or shear to improve the accommodation of the crystallites by allowing them to change shape more easily.

This implies that localised creep processes on the crystallite scale takes place in graphite immediately it is irradiated. The rate of creep decreases, passes through a minimum when the shape factor of the crystallites is most favourable, then rises again and continues to rise until basal plane micro-crack closure has taken place and an equilibrium rate of creep and bulk expansion of the graphite is approached. Also, because the ratios of c-axis to a-axis dimensional change are quite different in the cases of thermal expansion and irradiation, the CTE would not be expected to form a good basis for predicting irradiation shrinkage rates except where the crystallites have a low shear modulus and little strain.

3. EXPERIMENTAL

Graphite specimens (2.625 inches long and 0.22 inches diameter) representing both parallel and perpendicular cuts (with respect to crystallite orientation) from some 14 graphites were irradiated in the Dragon Reactor.

These graphites represent most of those selected for a broadly-based test programme following a review of state of knowledge made during the summer of 1965. It was decided at this time that from the viewpoint of eventually producing a specification for radiation stable graphites for power reactor use, the programme should be built around well graphitised isotropic graphites of both high and low CTE although some anisotropic materials should be included in the interests of reaching a deeper understanding of the underlying mechanisms.

The specimens were contained in hollow fuel-spine containers which were stacked within the vertical arrangements of annular fuel compacts in the reactor. Nickel and iron flux monitors were included in special recesses in the spine containers.

The typical initial physical properties of the graphites are given in Table 1. Of these graphites, 5 were "pressed" graphites and the remaining 11 were extruded graphites. The graphites have been divided into two groups; the first group consists of "improved" isotropic graphites of high CTE; 5 of the 7 graphites in this group were based on gilsonite (a spherical grist particle with a spherical arrangement of crystallites, prepared from a naturally occurring pitch of globular form). The second group contains a

Table 1

List of Graphites and their Physical Properties

Ref. No.*	Density ρ g cm^{-3}	Young's Modulus E 10^6 psi	Electrical Resistivity R m ohm cm^{-1}	Crystallite Height L_c Å	Coefficient Thermal Expansion (20-400°C) CTE 10^{-6} °C^{-1}	p = Pressed e = Extruded	
17 //	1.73	1.30	0.80	236	4.40	e	Isotropic, gilsonite based
⊥		1.11	0.91		4.96		
1 //	1.80	1.17	0.91	317	4.78	p	Isotropic, gilsonite based
⊥		1.08	0.96		4.98		
16 //	1.80	1.40	0.74	397	4.0	e	Isotropic, gilsonite based
⊥		1.25	0.87		4.5		
21 //	1.6	1.55	1.0	300	4.9	e	Isotropic, gilsonite based
⊥		1.51	1.1		5.1		
6 //	1.68	1.11	1.77	237	4.9	e	Isotropic pitch coke
⊥		0.93	1.82		5.4		
7 //	1.88	1.72	0.77	306	4.06	e	Isotropic
⊥		1.61	0.84		4.59		
5 //	1.75	1.90	0.80	359	4.52	e	Isotropic gilsonite based
⊥		1.78	0.85		4.74		
59 //	1.78	1.93	0.48	440	1.3	e	P.G.A.
⊥		0.88	0.91		3.2		
34 //	1.80	1.60	1.47	333	3.7	p	P.2239 high strength graphite (used for top blocks of Dragon fuel element)
⊥		1.30	1.49		3.9		
2 //	1.66	1.27	0.60	618	2.04	p	
⊥		0.96	0.71		2.55		
37 //	1.75	1.37	0.93	512	2.58	p	
⊥		0.96	1.13		3.01		
18 //	1.73	1.50	0.97	510	2.55	p	
⊥		0.97	1.23		3.68		
60 //	1.74	1.50	1.02	382	2.0	e	Dragon G5 (used for Dragon fuel tubes)
⊥		1.18	1.68		3.75		
62 //	1.78	1.95	0.73	557	1.3	e	HX-30 (used for Dragon fuel tubes)
⊥		0.88	1.30		2.9		

*The symbols // and ⊥ refer to the grain orientation.

range of graphites including anisotropic graphites such as PGA and near isotropic graphites such as No. 34.

The temperatures of the specimens were derived in part from thermocouples in adjacent elements in the core but mainly from correlating the shrinkage data for well characterised materials (such as graphite No. 60) in the HFR reactor Petten, against the shrinkages found for the neutron doses (~3 x 10^{20} n cm^{-2}) experienced by the specimens in Dragon. Monte-Carlo type calculations by Reed [9] have established that the graphite damage factor for the Dragon/THTR capsule in HFR Petten is comparable to that in Dragon. For Ni dose measurement the following relationship holds:

Ni dose Dragon = Ni dose Petten HFR (Dragon/THTR capsule) = 1.7 Ni dose Dido

4. RESULTS

The irradiation shrinkages of a given graphite were plotted against height in the reactor core. The smooth curve drawn through these points is complex because of the differing temperature and flux axial profiles in the core. However using the temperature profile (900-1200°C) which was established by the behaviour of well characterised materials, the shrinkage of each material has been obtained for temperatures of 900°C (where the data is sufficiently accurate) 1000, 1100 and 1200°C with neutron doses (Ni) which range from 2.4 to 3.3 x 10^{20} n cm^{-2}. The average rates of shrinkage per Ni dose of 10^{20} n cm^{-2} can then be obtained.

For an extruded anisotropic graphite only one direction of cut has a predominately in plane orientation of the crystallites and the volume change of the material is given by:

$$\frac{\Delta V}{V} = \frac{\Delta L_{//}}{L_{//}} + \frac{2\,\Delta L_{\perp}}{L_{\perp}}$$

For a pressed graphite because any isotropy results in alignment of crystallites within a plane (i.e., 2 directions of cut) the volume change is given by:

$$\frac{\Delta V}{V} = \frac{2\,\Delta L_{//}}{L_{//}} + \frac{\Delta L_{\perp}}{L_{\perp}}$$

where the subscripts // and $\perp$ refer to <u>crystallite orientation</u> and not necessarily to direction of extrusion or pressing.

The average rates of volume change of the 14 graphites per unit Ni dose of 10^{20} n cm^{-2} over a range 0-3 x 10^{20} n cm^2 are given in Fig. 4 on a log $\frac{\Delta V}{V}\%$ against $\frac{10^4}{T}$ °K plot.

In Table 2 the average rates of volume shrinkage at 1200°C for the graphites are tabulated together with the weighted mean physical properties of the materials (i.e., $\frac{1}{3}$ // + $\frac{2}{3}$ ⊥ for and extruded graphite and $\frac{2}{3}$ // + $\frac{1}{3}$ ⊥ for a pressed graphite). In this way the irradiation shrinkages of a wide range of graphites can be correlated with their physical properties without involving the complexity of anisotropy.

Following the theoretical model of mechanical crystallite/crystallite interaction developed in Section 2, values of $R_M L_c$ (i.e., the product of the mean electrical resistivity R_m expressed in mΩ cm and L_c expressed in Angstrom units) should provide a parameter which is related to the ratio $\frac{L_c}{L_a}$ because it can be argued that the electrical resistivity is related to the crystallite diameter, i.e., $R = K \frac{1}{L_a}$ where K is some constant. A plot of the average rates of volume shrinkage against the parameter $R_M L_c$ is shown in Fig. 5. It can be seen that there is a fair degree of correlation, i.e., the smaller the parameter, the smaller the shape factor or height/diameter ratio and the smaller the rate of shrinkage. In Fig. 6 another parameter $E_M R_M L_c$ is plotted against the average rates of shrinkage. This plot gives a better correlation and shows that the ability of crystallites to shear or strain (i.e., those graphites which have a low Young's Modulus) results in a lower rate of shrinkage.

5. DISCUSSION

In Section 2 the hypothesis has been advanced that the CTE of a graphite provides only an approximate basis for predicting the irradiation shrinkage of a graphite because of the wide difference in ratio of crystallite c-axis and a-axis dimensional change in the two processes. The difference in ratio, (+30c:+1a for CTE in contrast to +2c:-1a for irradiation above 500°C) places much more emphasis on the shape factor $\frac{L_c}{L_a}$ and on the ability of the crystallite to deform by shear, in the case of irradiation. A plot of volume irradiation shrinkage at 1200°C against mean linear CTE is given in Fig. 7(b) and it can be seen that the correlation is not very good. For example graphites 1 and 5 have similar CTE's of 4.9 and 4.7 x 10^{-6} $°C^{-1}$ respectively and therefore Simmons accommodation coefficients of 0.21 and 0.22. Applying the PGA crystallite shrinkage rates shown in Fig. 1 the predicted volume shrinkage rates for graphites 1 and 5 are 0.19% and 0.175% per 10^{20} n cm^{-2} (Ni dose Dragon) respectively, whereas the actual rates are 0.27% and 0.46%. It is obvious that graphite 5 would have to have a very low accommodation factor because it is shrinking at near that rate which would result from pure a-axis character in all 3 directions (i.e., 0.51% $\frac{\Delta V}{V}$) if the PGA crystallite dimensional changes are to be applied through Equation (2).

The difference between the observed irradiation shrinkage rates of graphites 1 and 5 can be accounted for by considering the effect of the less

T

Table 2

Average Rates of Volume Shrinkage at 1200°C and Mean Physical Properties of Graphites

Ref No.	Mean Physical Properties					$E_M R_M L_c$	$\frac{\Delta V}{V}\%$ 10^{20} n cm^{-2} at 1200°C	Isotropy Ratios			
	CTE_M x 10^{-6} °C^{-1}	E_M x 10^{-6} psi	R_M m ohm^{-1}	L_c Å	$R_M L_c$			Irradiation	Pre-Irradiation		
									E	R	CTE
1	4.91	1.13	0.94	317	296	333	0.273	1.11	1.02	1.05	1.04
17	4.78	1.17	0.88	236	217	254	0.323	1.14	1.07	1.04	1.13
16	4.34	1.30	0.82	397	326	423	0.350	1.17	1.12	1.18	1.12
6	5.23	0.99	1.80	237	423	420	0.366	1.45	1.19	1.14	1.14
7	4.41	1.65	0.81	306	248	410	0.379	1.68	1.07	1.09	1.13
21	5.0	1.52	1.06	300	318	480	0.447	1.19	1.03	1.10	1.04
5	4.67	1.82	0.83	359	297	540	0.458	1.14	1.07	1.06	1.05
59	2.6	1.23	0.77	440	340	417	0.346	1.57	2.22	1.8	2.45
2	2.25	1.16	0.63	618	390	453	0.442	1.15	1.32	1.18	1.25
34	3.8	1.50	1.48	333	493	737	0.504	1.25	1.23	1.01	1.05
37	2.72	1.28	1.07	512	547	700	0.576	1.14	1.43	1.22	1.17
18	2.93	1.33	1.06	510	540	720	0.624	1.40	1.54	1.27	1.45
60	3.17	1.3	1.46	382	558	724	0.643	1.48	1.27	1.50	1.87
62	2.4	1.23	1.11	552	620	760	0.654	1.37	2.27	1.78	2.23

compliant crystallites in graphite 5. The relatively high value of Young's Modulus in graphite 5 results in a higher rate of irradiation shrinkage because the crystallites are not strained or plastically deformed to the degree which exists in graphite 1. (In Fig. 3, compare point P_1 for graphite 5 and point P_1' for graphite 1). The two graphites can have more or less the same CTE because this physical property depends largely on the yield point of the crystallites in the c-axis direction (with consequent formation of basal plane microcracks) and only to a small extent on the crystallite diameter (L_a) and Young's Modulus. There is thus a general correlation to be expected between CTE and L_c and this is shown in Fig. 7(a) for the 14 graphites. A low CTE implies a lower c-axis yield point for the crystallites, a larger L_c and a greater degree of microporosity in the form of microcracks. The microcracks relieve some of the c-axis tensile stresses and thereby reduce the a-axis compressive forces to which the crystallites are subject. It is possible that a vestigial microcrack system providing some accommodation for a-axis expansion is set up. The initial expansion effects of a graphite found in the early stages of irradiation may be related to extensions of the microcrack systems initiated by relief of strain. These initial expansion effects are only very transient at high temperature, a neutron dose of $\sim 0.5 \times 10^{20}$ n cm^{-2} completes the effect at 1200°C but at lower temperatures the effect persists (as an increasing rate of shrinkage) for as long as 10^{21} n cm^{-2} at 900°C. (See Fig. 8). The initial expansion effect appears to be larger for a high CTE graphite than for a low CTE graphite, (e.g., ca. 600°C) and again may be explained as a release of greater crystal strain and an extension of the microcrack system which is initiated by irradiation.

Under irradiation, the crystal strain energy can be regarded as the motive force for localised creep on the crystallite scale. The crystallite shape changes caused by irradiation reduce the strain at first and the creep passes through a minimum when the crystallite shape factor is at its most favourable (P_6 in Fig. 3), i.e., the closest approximation to the original crystallite shape before cooling from ~2000°C during manufacture. At this stage the rate of shrinkage is a maximum, i.e., the non-accommodated c-axis component is at a minimum. Thereafter the rate of shrinkage must fall and the crystallite must deform by shear if the graphite is not to start expanding rapidly. At high neutron doses the basal plane microcrack systems when closed by c-axis expansion of the crystallites create a new stress system which must expand the graphite, although the rate again may depend very much on the ability if the crystallites to shear or to undergo stress orientated growth, i.e., another creep system is created.

Further examination of the results presented in Fig. 6 shows that, for example, the relatively low rate of volume shrinkage of graphite 2 can be explained in terms of the low electrical resistivity and low Young's Modulus which compensate for the high L_c value of 618 Å, i.e., the graphite contains relatively large crystallites which can shear easily. On the other hand graphite 34 appears to have very unfavourable physical properties but does not shrink quite as fast as the present model suggests. One possible extension of the model is to take into account the change in Young's Modulus which takes place during irradiation. It is probable that the defect population impedes the ability of the crystallites to shear and that the rate at which Young's

Modulus changes with neutron dose is not the same for all the graphites considered. Preliminary results confirm that the fractional changes in Young's Modulus are dissimilar in many cases.

The experimental results do seem to confirm however that from the point of view of irradiation volume shrinkage, graphites containing crystallites with a low aspect ratio $\left(\frac{L_c}{L_a}\right)$ shrink less rapidly than those with a high aspect ratio and that graphites with a low Young's Modulus shrink less rapidly than those with a high Young's Modulus.

In other words a graphite should have low L_c (i.e., high CTE), low electrical resistivity (high L_a) and low Young's Modulus if it is to have a low rate of volume shrinkage. Once the volume shrinkage has been established, the bulk anisotropy of the material can be treated as another problem which merely distributes the shrinkage between the three major axes. Bearing in mind whether the material is in the "extruded" or "pressed" category, the linear CTE's can be used in conjunction with the Simmons equations to distribute the dimensional change appropriately in the absence of actual irradiation data. It will be seen from Table 2 that apart from some of the more isotropic graphites the irradiation isotropy ratio does not always correlate particularly well against any of the physical property anisotropy ratios or even any combination of them, graphite 7 presents a problem for example and further investigation is required.

It is considered that the volume shrinkage on irradiation represents a more basic property of the graphite and should be "understood" first before becoming involved in questions of linear dimension change and anisotropy.

For reactor applications the behaviour of a graphite under irradiation at various temperatures is required for neutron doses of up to 10^{22} n cm^{-2} Ni dose Dragon. Taking graphite 60 (Dragon G5) as an example, the irradiation behaviour of this anisotropic graphite has been reported by Blackstone for neutron doses of up to 2 x 10^{21} n cm^{-2} (Ni dose Dragon) and temperatures of 600, 900 and 1200°C. The volume changes of this material are plotted in Fig. 8(a), where the full lines represent the available data and the dotted lines an estimated extrapolation to higher doses. It is illogical to consider the average rate of shrinkage as has been customary, it is obviously more correct to consider the instantaneous rate of change taking place at a given neutron dose and temperature. The curves in Fig. 8(a) are differentiated in Fig. 8(b) and it is suggested that future quantitative models of graphite irradiation shrinkage should aim to provide equations which describe the instantaneous rates of volume change in terms of temperature, neutron dose and physical properties or initial shrinkage behaviour. For example it may be found that a combination of three exponential terms will generate the curves in Fig. 8(b) alternatively, a combination of c-axis and a-axis crystallite dimensional change contributions may be considered. It may be, as is suggested in Fig. 8(b), that the initial rates of shrinkage of a graphite are not necessarily related to the rates of expansion at higher doses in which case a graphite selected because of its low initial shrinkage rate may expand at a higher rate at higher neutron doses than a graphite

with a higher initial shrinkage rate. This is an area of study which requires much more attention.

6. SUMMARY AND CONCLUSIONS

Considering the volume behaviour of a graphite:

(i) The CTE is inversely related to the L_c.

(ii) The initial rate of irradiation shrinkage is related to $E_M R_M L_c$ where E_M is the "mean" Young's Modulus and R_M the "mean" electrical resistivity. $E_M R_M L_c$ is considered related to $E_M \left(\frac{L_c}{L_a}\right)$ (i.e., E_M . aspect ratio of the crystallites).

(iii) Different physical properties of the crystallites are important in thermal contraction and irradiation shrinkage and therefore CTE does not necessarily correlate with irradiation shrinkage rate.

(iv) The ability of the crystallites to yield in the c-axis direction during cooling after graphitisation is important in producing a high CTE (low L_c) and the ability to shear is less important. In irradiation shrinkage the ability to shear is important and the yield point is relatively unimportant.

(v) A low crystallite aspect ratio $\left(\frac{L_c}{L_a}\right)$ results in a lower rate of irradiation shrinkage because in a unit element of length the magnitude of crystallite/crystallite dimensional interaction is smaller for a low L_c and fewer in number for a large L_a. Also rates of crystallite dimensional change are slower for a large L_a.

(vi) Creep on a localised crystallite scale takes place all the time in graphite under irradiation and passes through a minimum at the maximum instantaneous rate of shrinkage.

7. REFERENCES

[1] D. R. de Halas, H. H. Yoshikawa. Proceedings 5th Conference on Carbon, Vol. 1, p.251, Pergamon Press, Oxford (1962).

[2] W. C. Morgan, Carbon 4, 215, (1966).

[3] J. H. W. Simmons, "Radiation Damage in Graphite," pp.138 and 144. Pergamon Press, Oxford 1965.

[4] R. J. Price, J. C. Bokros. J. Appl. Phys. 36 1897 (1965).

[5] R. J. Price, J. C. Bokros. Carbon 5, 73 (1967).

[6] H. Bridge, B. T. Kelly, P. T. Nettley. Carbon 2, 92 (1964).

[7] R. Blackstone, L. W. Graham, "Dimensional Changes in Graphite during High Temperature Irradiation in the HFR Petten." D.P. Report 473.

[8] J. B. Nelson, D. P. Riley. Proc. Phys. Soc. 5.

[9] D. L. Reed, "The Comparison of Carbon-Atom Displacement Rate in Graphite in the Dragon Reactor, the Petten HFR and a Low Enrichment HTR." D.P. Report 559.

[10] M. R. Everett, D. Lamb, Dragon Project Report to be Published.

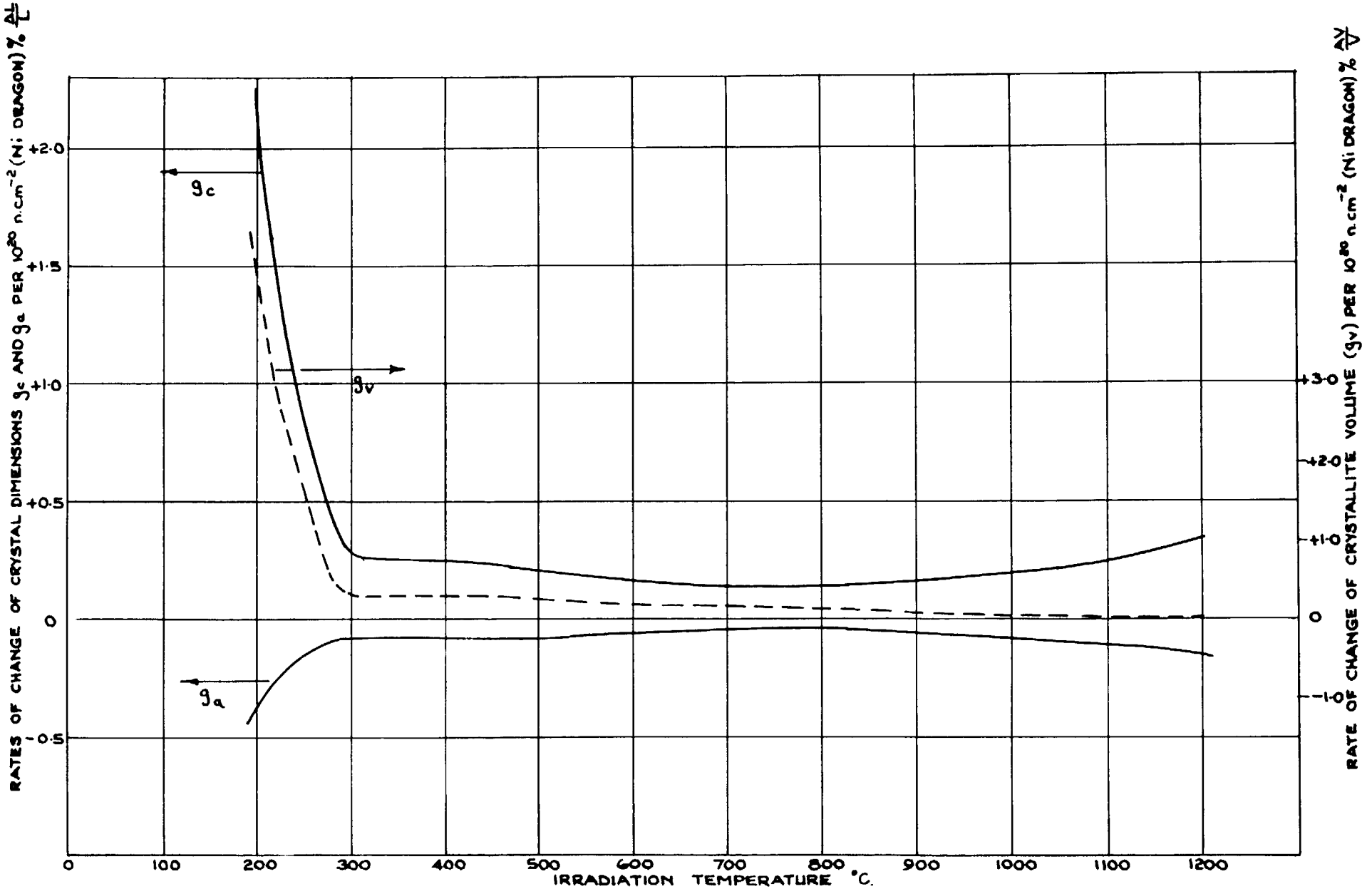

FIG. 1 RATES OF DIMENSIONAL CHANGE OF C-AXIS (g_c) a-AXIS (g_a) AND VOLUME (g_v) OF CRYSTALLITES IN PGA GRAPHITE PER UNIT NEUTRON DOSE OF 10^{20} n.cm^{-2} (Ni DRAGON) FOR TEMPERATURE RANGE 200-1200 °C. (AFTER BRIDGE et al AND GRAHAM)

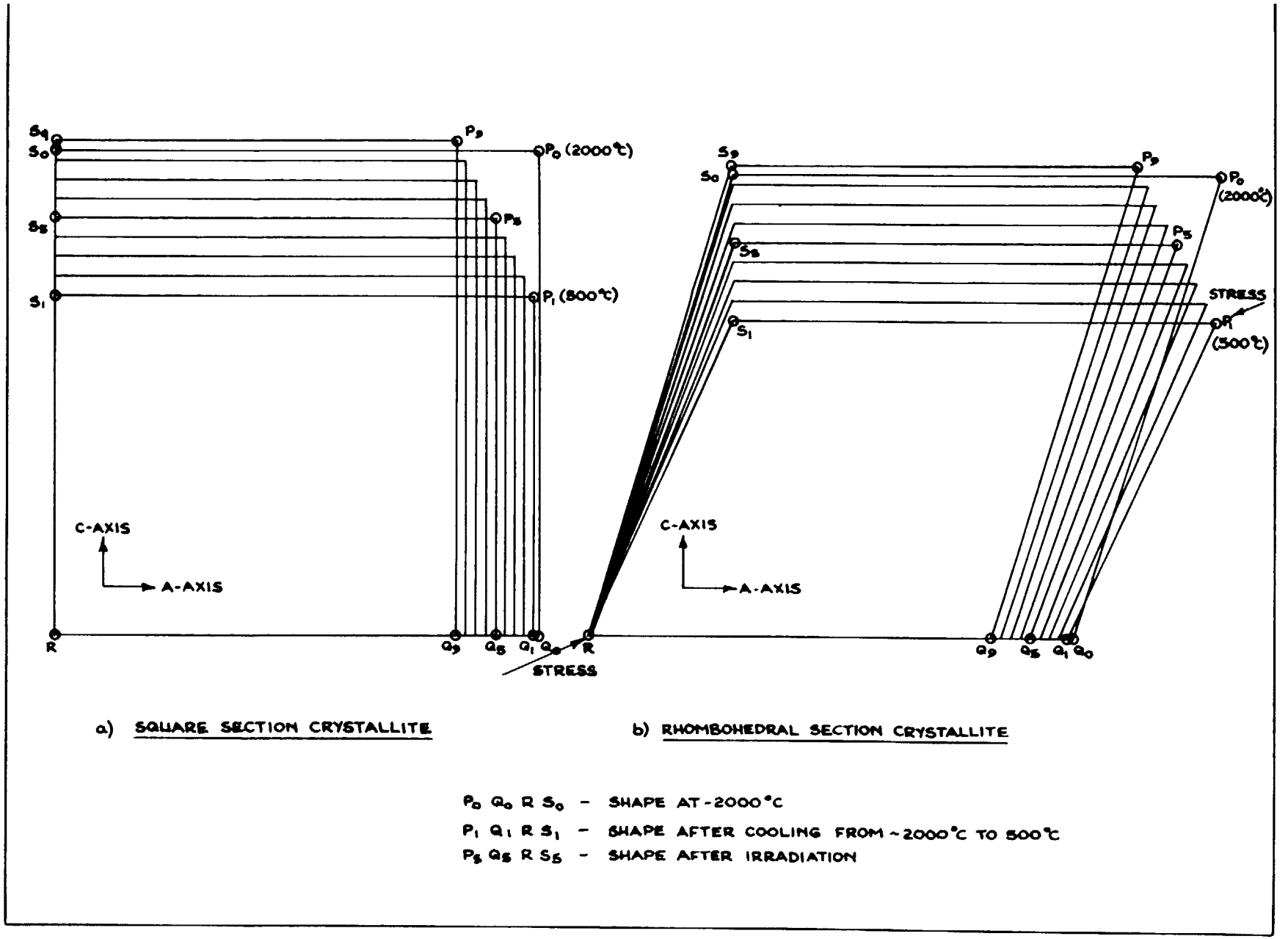

FIG. 2 SHAPE CHANGES OF HYPOTHETICAL CRYSTALLITE FORMS UNDERGOING THERMAL SHRINKAGE FOLLOWED BY IRRADIATION

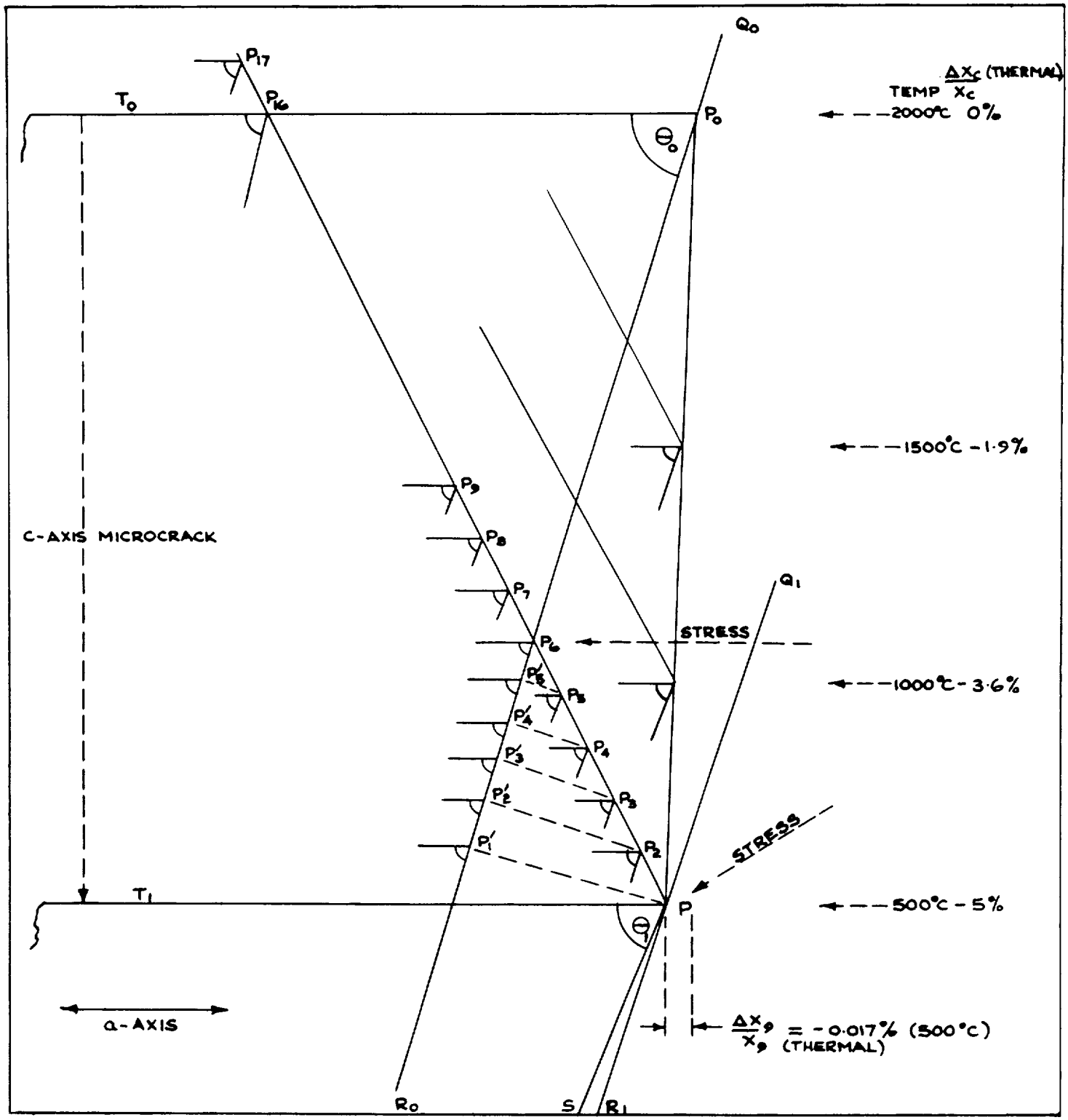

FIG. 3 TWO DIMENSIONAL DIAGRAM ILLUSTRATING CRYSTALLITE / CRYSTALLITE MECHANICAL INTERACTION FOLLOWING THERMAL SHRINKAGE AND IRRADIATION

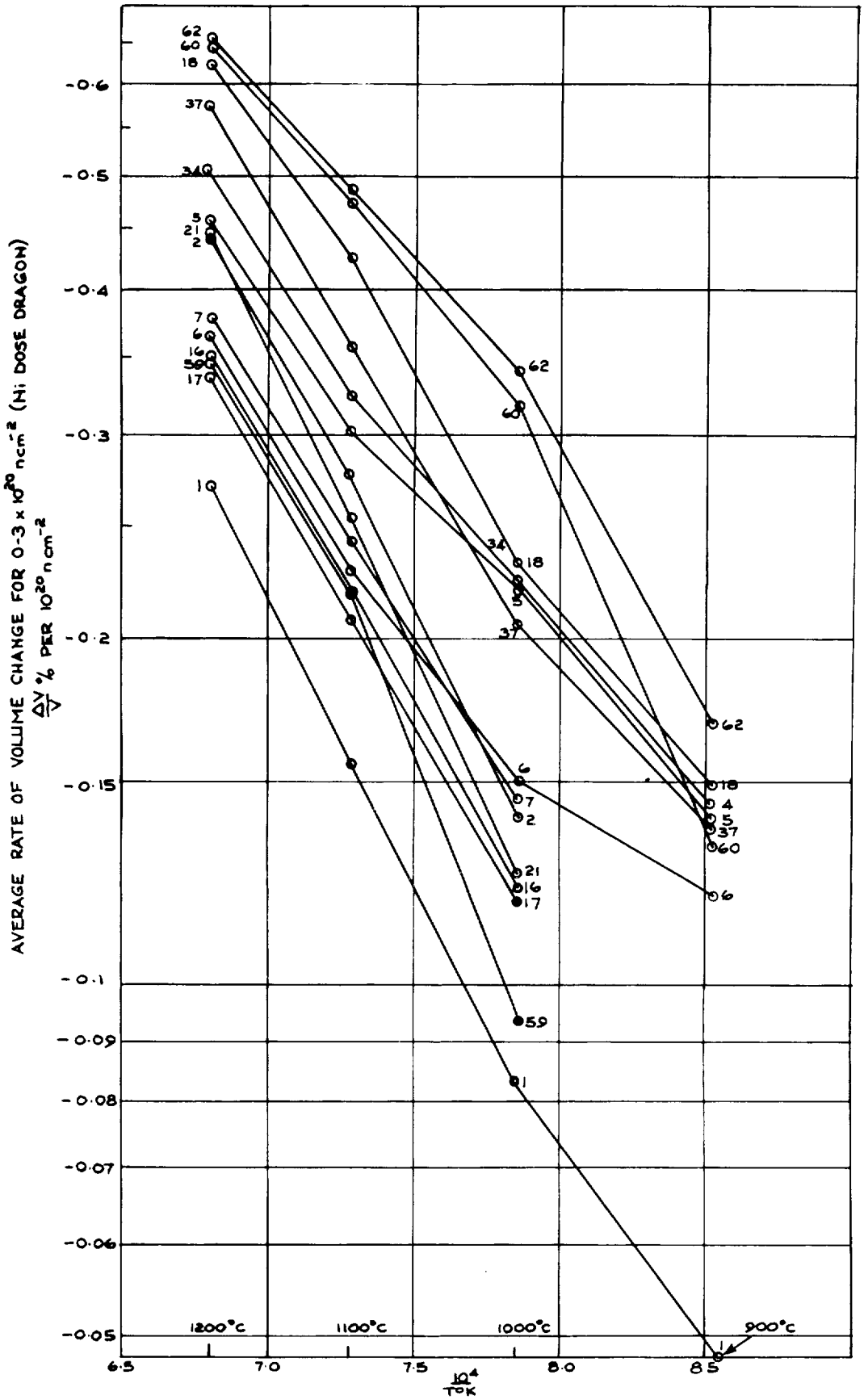

FIG. 4 LOG AVERAGE RATES OF VOLUME SHRINKAGE AGAINST $\frac{10^4}{T°K}$ $0{\cdot}3 \times 10^{20}$ n.cm^{-2} (Ni DOSE DRAGON)

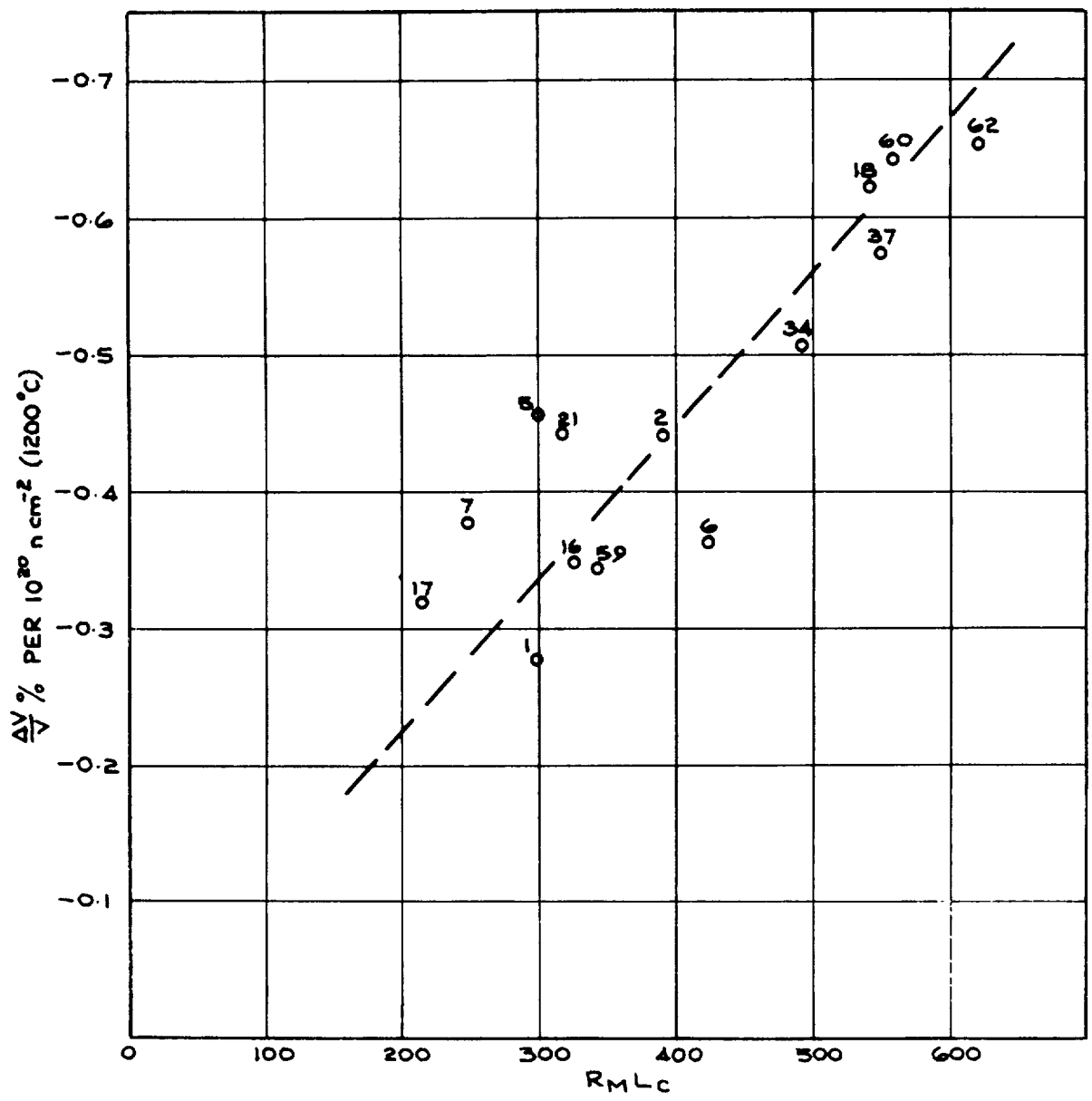

FIG. 5 PLOT OF RATE OF VOLUME CHANGE AGAINST PARAMETER $R_M L_C$

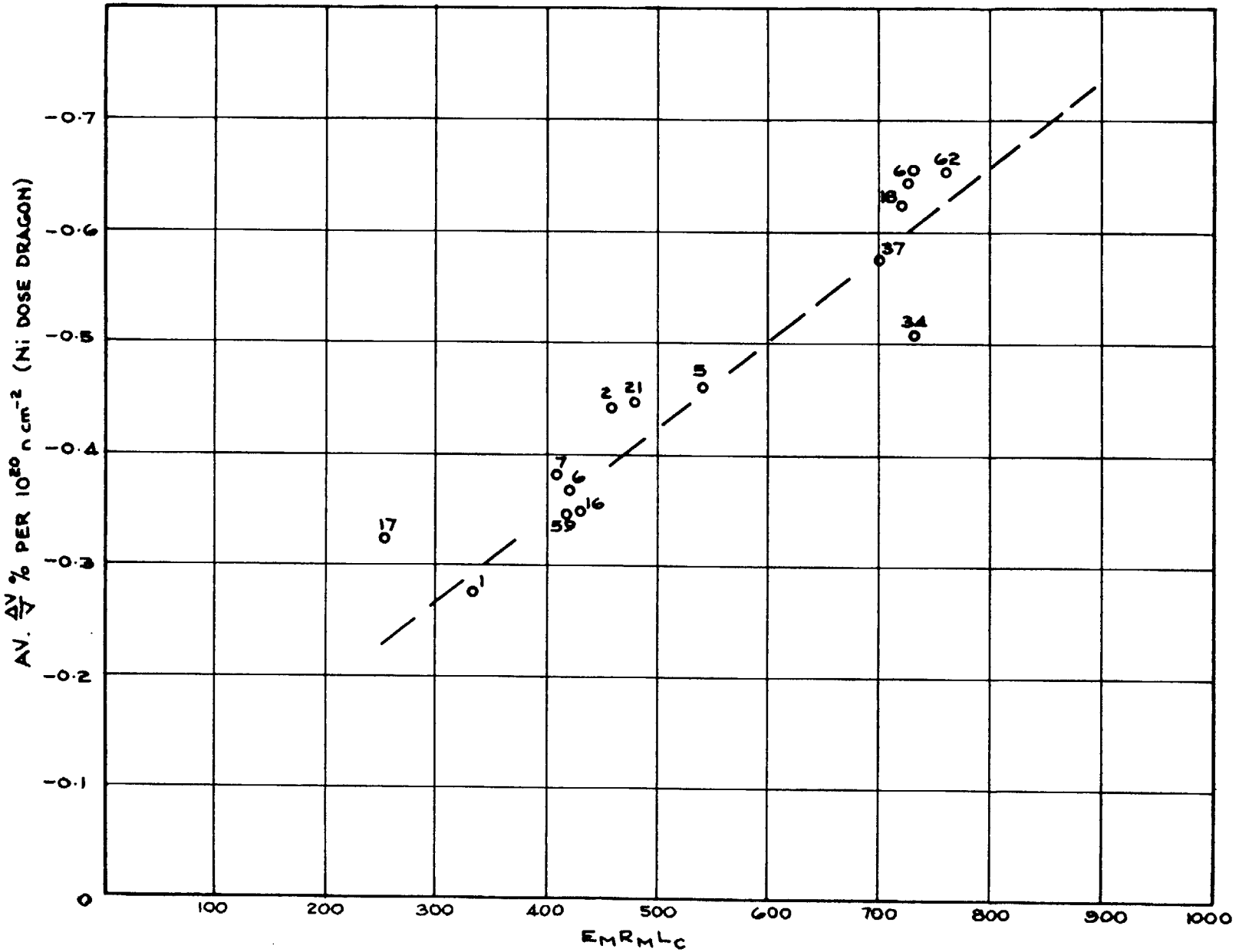

FIG. 6 PLOT OF AVERAGE RATE OF VOLUME CHANGE AGAINST PARAMETER $E_M R_M L_C$ (FOR 1200°C)

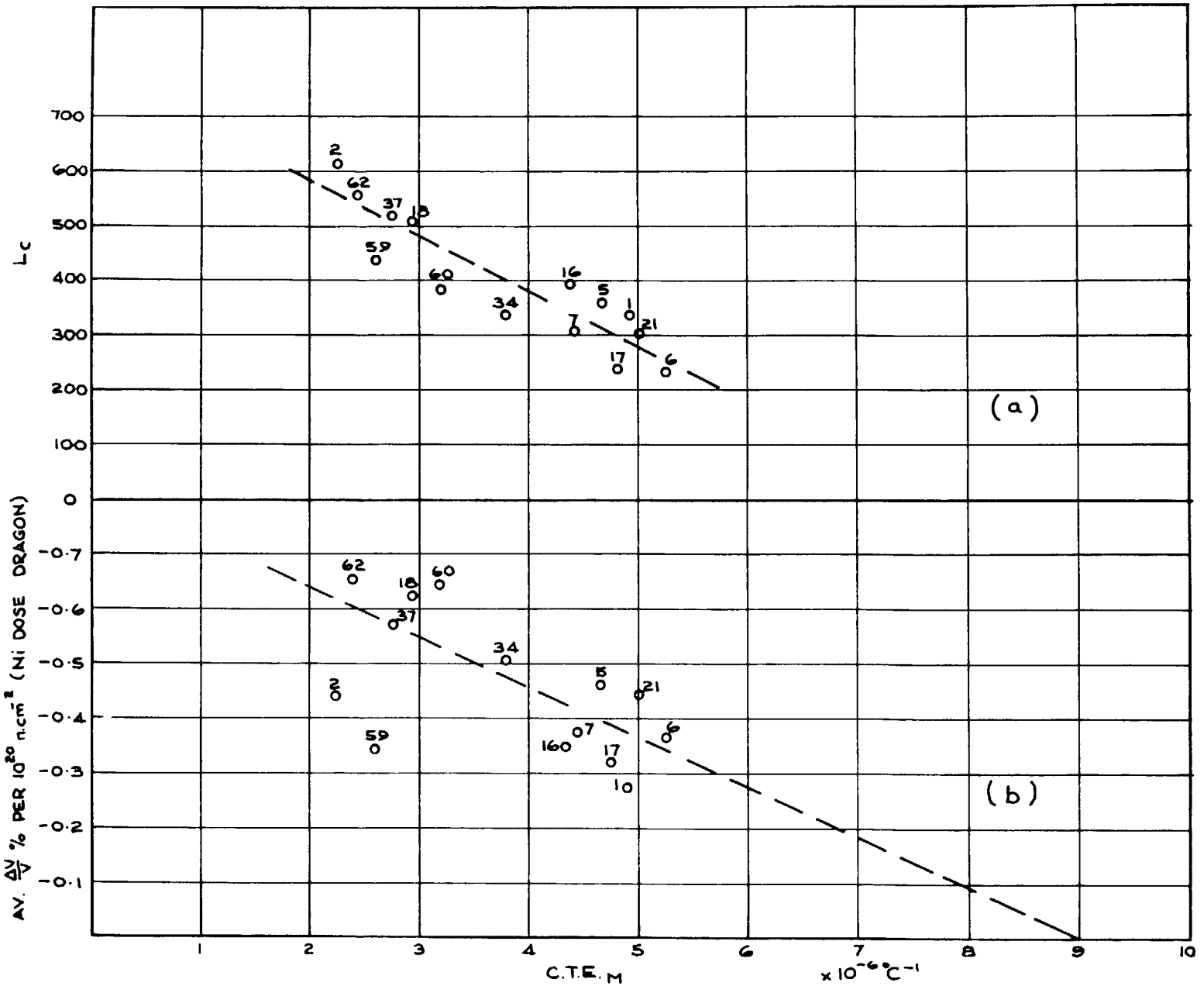

FIG. 7 PLOTS OF CTE_M AGAINST (a) L_C AND (b) RATES OF VOLUME CHANGE AT 1200 °C UNDER IRRADIATION

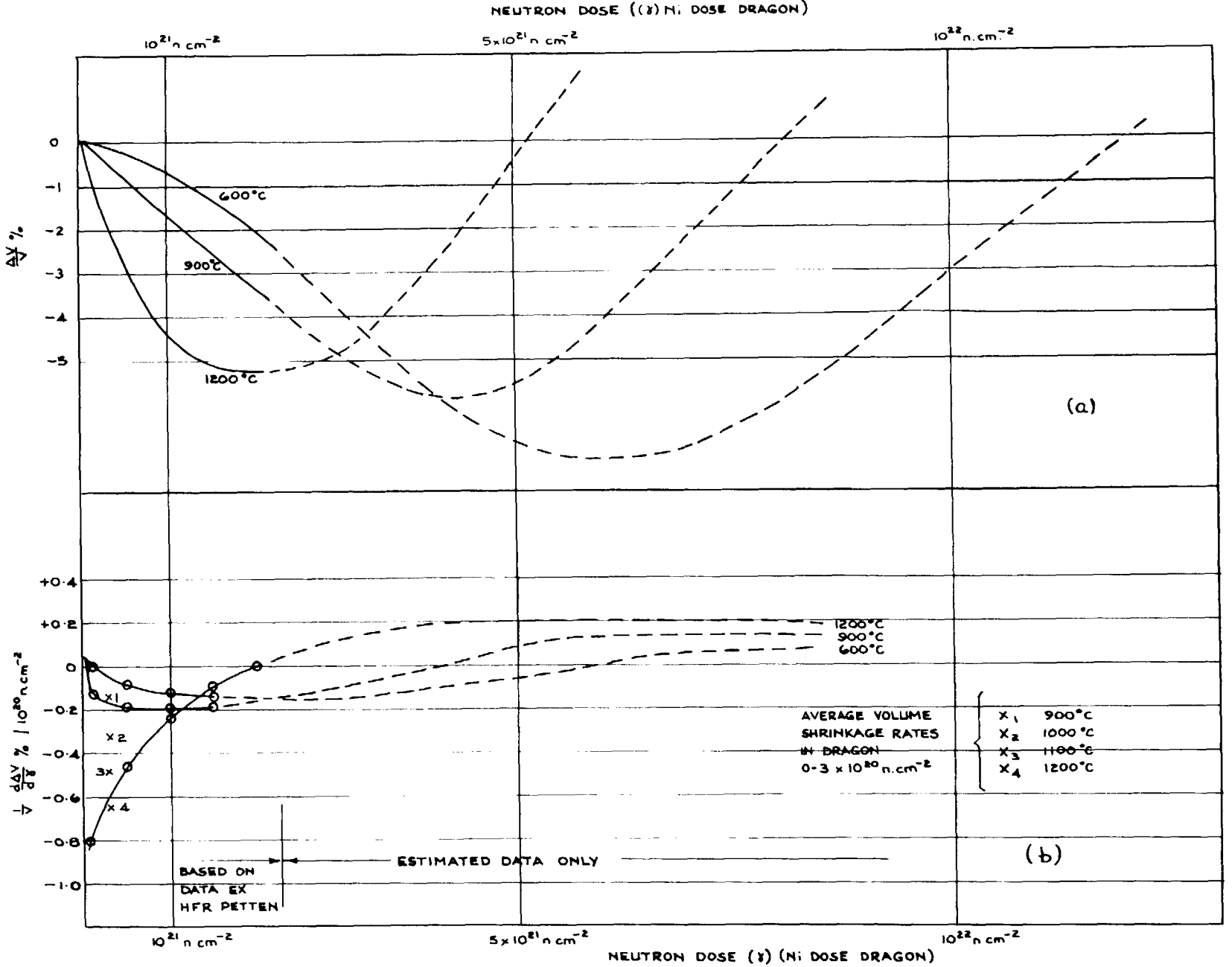

FIG. 8 VOLUME CHANGES (a) AND INSTANTANEOUS RATES OF VOLUME CHANGE (b) OF GRAPHITE Nº 60 AGAINST NEUTRON DOSE